

Metal-semiconductor fluctuation in the Sn adatoms in the Si(111)-Sn and Ge(111)-Sn ($\sqrt{3} \times \sqrt{3}$)R30° reconstructions

M. Göthelid

CRMC2, Centre National de la Recherche Scientifique, Campus de Luminy, Case 913, F-13288 Marseille Cedex 09, France

M. Björkqvist and T. M. Grehk

Department of Physics, Materials Physics, Royal Institute of Technology, S-10044 Stockholm, Sweden

G. Le Lay*

CRMC2, Centre National de la Recherche Scientifique, Campus de Luminy, Case 913, F-13288 Marseille Cedex 09, France

U. O. Karlsson

Department of Physics, Materials Physics, Royal Institute of Technology, S-10044 Stockholm, Sweden

(Received 16 June 1995)

The two components of the Sn 4*d* core level in the Si(111)-Sn and Ge(111)-Sn ($\sqrt{3} \times \sqrt{3}$)R30° structures are proposed to arise from semiconductor-metal fluctuations in the Sn adatom layer. Adsorption of potassium on the Si(111)-Sn ($\sqrt{3} \times \sqrt{3}$)R30° surface suppresses the metallic component and shifts the tin into a purely semiconducting phase with a filled dangling bond state.

Adsorption of tin on the (111) surface of the elemental group-IV semiconductors Si and Ge induces metallic T_4 (i.e., the threefold-hollow site directly above second-layer atoms) ($\sqrt{3} \times \sqrt{3}$)R30° reconstructions in certain coverage and annealing temperature regimes.^{1,2} Studies using scanning tunneling microscopy (STM) have, in combination with results from other techniques, revealed an almost homogeneous tin adatom layer where the number of substitutional Si or Ge adatoms varies with the detailed preparation.^{3,4} The highly perfect top layer is expected to be manifested by a single Sn 4*d* core-level component. Several experiments have however, shown that the Sn 4*d* core level is composed of at least two components in the tin-induced $\sqrt{3}$ structures.⁵⁻⁷ The origin of these peaks was briefly discussed by Göthelid *et al.*, where emission related to tin located in subsurface sites was excluded.⁵ Furthermore a defect-induced contribution was found to be unlikely due to the fact that the number of defects varies in a wide range with preparation while the core-level line shape did not vary substantially with preparation, provided that the $\sqrt{3}T_4$ phase was retained.^{5,6}

In the Si(111)-Sn system also a second $\sqrt{3}$ phase can be obtained, a semiconducting so-called mosaic structure comprising equal amounts of Si and Sn adatoms (see, e.g., Ref. 3). A charge transfer from the Si adatom to the Sn adatom dangling-bond state was concluded from voltage-dependent STM images.³ A similar charge transfer was also proposed for an analogous mosaic phase induced by Pb on the Si(111) surface.⁸ Core-level photoelectron spectroscopy (PES) on the Si(111)-Sn mosaic phase uncovered a single Sn 4*d* component coinciding with the low binding-energy peak of the T_4 Sn 4*d* core-level spectrum.⁶

In this paper we present core-level PES results from the Si/Sn T_4 and Ge/Sn T_4 and from the Si/Sn mosaic $\sqrt{3}$ structures. In order to elucidate the intriguing issue of the origin of the different contributions in the Sn 4*d* core-level spectra

we use K adsorption as a probe/perturber of the surface electronic structure. The room-temperature adsorption of K transforms the two-component Sn 4*d* level of the T_4 structure to a mosaiclike single-peak line shape. In coincidence with the narrowing of the Sn 4*d* the Gaussian width of the Si 2*p* core level decreases drastically, and the metallic surface turns semiconducting. We interpret the two tin components to be due to Sn being in a metallic or in a semiconducting state. The fluctuations between the two states are manifested by a very large width of the Si 2*p* core-level peak related to Si below the Sn adatoms. The deposition of potassium confines the tin to the semiconducting phase, where the Gaussian width of the Si 2*p* level is much smaller.

The experiments were performed at MAX-LAB (Lund, Sweden) using a modified SX-700 monochromator. The photoemission spectra were recorded by a 200-mm-radius hemispherical analyzer of Scienta type.⁹ In connection with the photoemission chamber is a preparation chamber comprising evaporation sources, sputtering equipment, a low-energy electron diffraction (LEED) optics, and sample heating. The experimental settings were chosen to give a resolution around 80 meV, as revealed from the Fermi edge of a tantalum foil in contact with the sample. Sharp (7×7) and $c(2 \times 8)$ LEED patterns were achieved after either annealing the pre-etched Si(111) sample at 900 °C or repeated cycles of Ar⁺-ion sputtering and annealing of the Ga-doped Ge(111) sample at 650 °C, measured with a pyrometer. During the annealing process the pressure was kept below 5×10^{-10} Torr. Cleanliness of the sample was checked with photoemission spectra from the O 1*s* and C 1*s* core levels and from the valence band, which showed strong surface states and extremely sharp Si 2*p* core levels.¹⁰

Tin was evaporated from a tungsten filament evaporator and K from a carefully outgassed chromate dispenser (SAES Getters S.p.A.). During evaporation the pressure was kept below 1×10^{-10} Torr.

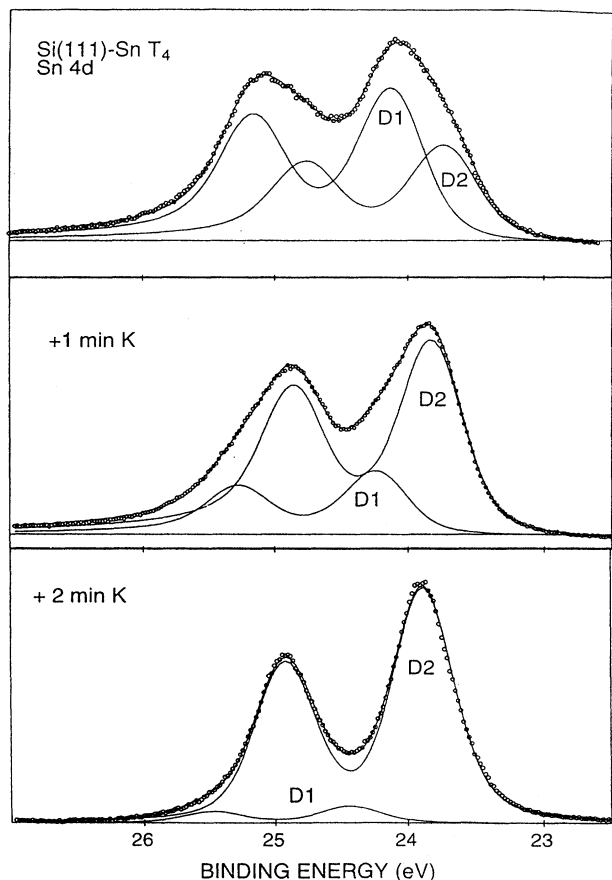


FIG. 1. Sn 4d core-level spectra from the Si(111)-Sn T_4 surface (a), after deposition of 1 min of K (b), and after 2 min K deposition (c). The photon energy used was 70 eV in all three spectra.

In Fig. 1 a set of Sn 4d core-level spectra from the clean Si(111)-Sn T_4 surface (a), after 1 min of K deposition (b), and after 2 min of K (c) is shown. As described above, the T_4 phases gives rise to two components in the Sn 4d core level. The intensity ratio is the same here as it is in the Ge(111)-Sn case, Fig. 2(a), although the stronger peak is on the low binding-energy side for the Ge/Sn surface while on the high binding-energy side in the Si/Sn case. Furthermore, the binding energies of the components are the same on the two surfaces.

When the amount of K on the surface increases, the Sn 4d core level sharpens and the high binding-energy peak fades as intensity is shifted from D1 to D2, see Fig. 1. The final line shape, obtained at $\sim \frac{1}{3}$ -ML K coverage,¹¹ resembles the one from the mosaic phase, shown in Fig. 2(b). The mosaic structure is not fully developed here but the spectrum contains in addition also a slight contribution from the T_4 reconstruction.

In Fig. 2(c) the Si 2p core-level spectrum from the mixed mosaic- T_4 phase is shown, where a four-component deconvolution was used, similarly to the Si(111)-Pb $\sqrt{3}$ mosaic phase.⁸ The three surface contributions, labeled S1, S2, and S3, respectively, were related to adatoms (S1), silicon directly below the Si adatoms (S2), and second-layer silicon

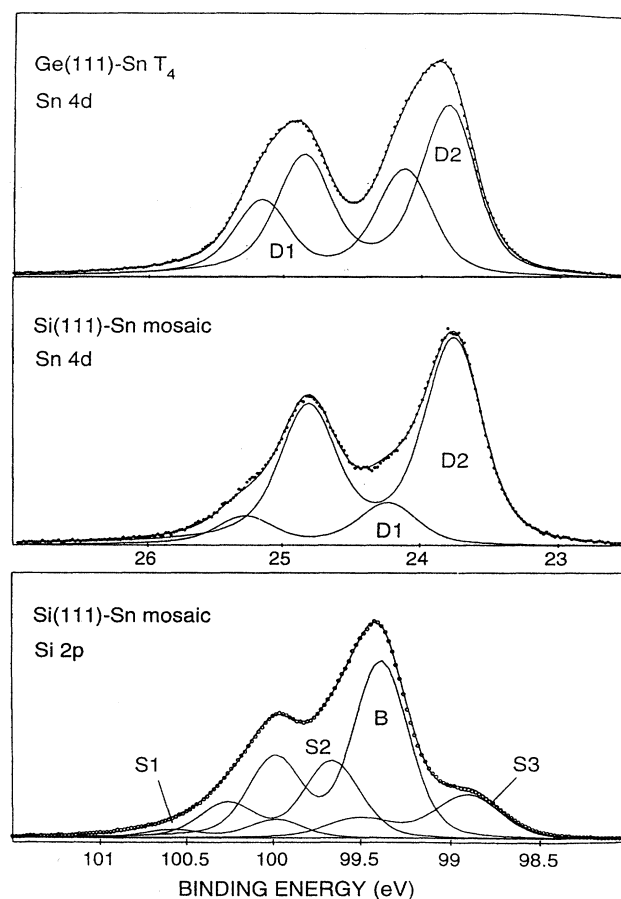


FIG. 2. Sn 4d core-level spectra from the Ge(111)-Sn T_4 (a) and the Si(111)-Sn mosaic (b) and a Si 2p spectrum from the mosaic phase (c), utilizing 70-eV photons in the case of the Sn 4d and 130 eV in the case of the Si 2p core-level spectra.

below the Pb adatoms (S3).⁸ So for the assignment of the surface-shifted peaks in the present Si 2p core-level spectra from the two tin-induced $\sqrt{3}$ surface reconstructions we use the same routine as applied to the Si/Pb case⁸ and thus relate S1 to Si adatoms, S2 to Si below the Si adatoms, and S3 to Si below the Sn adatoms.

If $I_2 + I_3 = 1$ ML (I denotes the intensity of the peaks) in the T_4 spectrum in Fig. 3(a), which should be the case if the assignment is correct, then $I_1 = 0.06$ ML, i.e., 18% substitutional Si adatom defects in the Sn adatom layer. This value is somewhat large but it is clearly within the limits set up in the work by Törnevik *et al.*,¹¹ which presents some support for the peak assignment.

The evolution of the T_4 reconstruction Si 2p core level with increasing K coverage is shown in Figs. 3(a)–3(c); the LEED pattern was $\sqrt{3}$ for all spectra shown here. The very weak adatom peak (S1), similar to S1 in the mosaic spectrum, Fig. 2(c), is seen on the high binding-energy side. The second surface peak (S2) has an intensity I_2 being 3.4 times I_1 , whereas I_3 is 11.4 times I_1 . After 1-min K deposition, i.e., about $\frac{1}{6}$ ML, the S1 contribution is no longer present as a separate peak in the spectrum, possibly due to a chemical

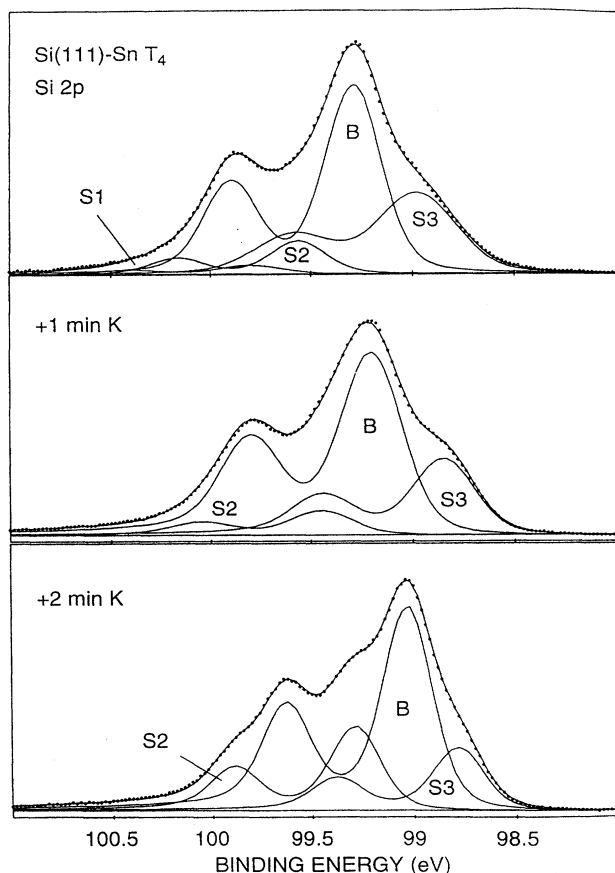


FIG. 3. A set of Si 2*p* spectra recorded at 130-eV photon energy, following the same sequence as Fig. 1.

shift of the adatoms to lower binding energy. S2 has increased slightly and thus probably also includes the former S1 contribution. The shift of the bulk peak to lower binding energy indicates an upward band bending induced by the potassium.

In the lower spectrum in Fig. 3(c), after 2 min of K evaporation, the surface peak intensity ratio has changed markedly. Still the total intensity of these peaks corresponds to 1 ML. The change in intensity ratio indicates that the K-saturated $\sqrt{3}$ surface is not a top-site K-terminated surface, at least not exclusively. One could imagine that the alkali metal enters into the surface geometry where it gives up an electron to fill the dangling bonds. The adsorbate, however, does not adopt the top site but presumably a subatom site which induces the observed structure of the Si 2*p* core level.

Noteworthy is also the Gaussian widths of the Si 2*p* surface peaks, and primarily S3, which before deposition of potassium is enormously large, 0.39 eV, in Fig. 3(a). This value is some 0.12 eV wider than the bulk peak width, 0.27 eV, of that spectrum. The remaining two surface peaks both have 0.32 eV Gaussian width. Attempts to fit the S3 peak with two separate components were made, but as we move on to the spectra recorded from the K-dosed surfaces there is no consensus in the peak evolution with this number of contributions. However, the S3 width decreases drastically after

1 min K deposition, and is in the spectrum in Fig. 3(b) equal to the S2 surface peak width. Finally, in the Si 2*p* spectrum from the saturated surface all peaks have the same width 0.23 eV at room temperature. As noted above the intensity ratio in the Si 2*p* spectra in Fig. 3(c) is not in agreement with the assignment of the surface peaks in Figs. 3(a) and 3(b), i.e., although the $\sqrt{3}$ structure is preserved the introduction of K on the surface changes the topmost Si layer electronic structure.

The question of the origins of the two Sn 4*d* peaks in the T_4 structures has still not been dealt with. The binding-energy position of D2 in the T_4 phase is the same as for D2 in the mosaic phase, where the Sn adatom dangling bonds are filled by electrons from adjacent Si dangling bonds. The single-peak Sn 4*d* core level from the semiconducting ($2\sqrt{3} \times 2\sqrt{3}$) surface displayed also the same binding energy,¹² and thus we find it tempting to assign D2 to Sn in a semiconducting form, while we assign D1 to metallic tin, based on the metallicity of the T_4 surfaces as revealed from the valence-band spectra.

Apparently the $\sqrt{3}T_4$ surface structure contains tin in both a metallic and a semiconducting state, which also affects the closest subsurface neighboring silicon atoms, manifested through the increased S3 width. One of the states is similar to the mosaic state where the tin dangling bond is filled by an electron from the Si dangling-bond state. One could imagine a mosaiclike scenario where some of the Sn adatoms act as electron donors and the rest are in the same electron acceptor state as they are in the mosaic phase. This situation would imply a semiconducting surface with obviously is not the case here. Moreover such a situation would clearly be observable in STM, if it is not a very rapid fluctuation of electrons from one Sn dangling bond to another, but still we would expect a semiconducting surface.

A more tempting situation is one where the adatoms are metallic to a larger extent and semiconducting a smaller fraction of the time. In the semiconducting state the dangling bond is filled while Sn in the metallic state has an unfilled dangling-bond orbital. Since all atoms appeared the same in STM,^{3,4} there must be a fluctuation of the electronic charge between the different dangling-bond states. The very large width of S3 can also be explained by this possible fluctuation since the Si beneath the Sn adatoms experiences adatoms in two different states, and thus may apprehend different core-level shifts.

The Ge(111)-Sn $\sqrt{3}$ surface also shows two peaks, in the same positions as D1 and D2 in the Si(111)-Sn $\sqrt{3}$ structure. The interchanged intensity of the peaks, as compared to Si/Sn, uncovers a preference for a semiconducting Sn adatom behavior in the Ge/Sn case. The reason for this can be found in a paper by Ewald¹³ where it was found that addition of a small amount of Ge, 0.75 wt %, stabilized the semiconducting phase of tin, and shifted the transition temperature to higher temperatures. The solubility of Si in Sn, or vice versa, is, on the other hand, practically equal to zero,¹⁴ and mixing-induced shifts of the kind observed for Ge-Sn can in that sense not be expected for the Si-Sn surface. Thus, growing tin on Ge can for that reason be expected to give a stronger predilection for the α phase on Ge than on Si as observed here. Moreover, the transition temperature was found to be

lowered by the application of hydrostatic pressure.¹⁵ The smaller lattice parameter of Si may in this respect give rise to a higher “pressure” on the Sn overlayer than Ge does. Hence also from this argument one might expect a more metallic overlayer on Si than on Ge.

In summary, we have studied the Sn-induced $\sqrt{3}$ reconstructions on the Ge(111) and Si(111) surfaces. Adsorption of potassium on the Si(111)-Sn $\sqrt{3}T_4$ surface confines the Sn 4*d* core level to one single component, related to Sn in a semiconducting phase, while a high binding-energy peak, assigned to metallic tin, disappears when K is deposited. Re-

sults from STM combined with strong variations in the widths of the Si 2*p* components suggest that there is a phonon-supported fluctuation between these two states, as the electrons oscillate between the adatom dangling bonds. The higher preference for the semiconducting phase on Ge(111) than on Si(111) was discussed.

We thank the MAX-LAB staff for their assistance. This work was supported by the Swedish Natural Science Research Council (NFR), the Swedish Research Council for Engineering Sciences (TFR).

* Also at UFR Sciences de la Matière, Université de Provence, Marseille, France.

¹P. J. Estrup and J. Morrison, *Surf. Sci.* **2**, 465 (1964).

²T. Ichikawa and S. Ino, *Surf. Sci.* **105**, 395 (1981).

³C. Törnevik, M. Göthelid, M. Hammar, U. O. Karlsson, S. A. Flodström, C. Wigren, and M. Östling, *Surf. Sci.* **314**, 179 (1994).

⁴M. Göthelid, M. Hammar, C. Törnevik, U. O. Karlsson, N. G. Nilsson, and S. A. Flodström, *Surf. Sci.* **271**, L357 (1992).

⁵M. Göthelid, T. M. Grehk, M. Hammar, U. O. Karlsson, and S. A. Flodström, *Surf. Sci.* **328**, 80 (1995).

⁶C. J. Karlsson, E. Landemark, Y. C. Chao, and R. I. G. Uhrberg (unpublished); C. J. Karlsson, Ph.D. thesis, Linköping University, 1994.

⁷G. LeLay, J. Kanski, P. O. Nilsson, and U. O. Karlsson, *Appl. Surf. Sci.* **56-58**, 178 (1992).

⁸C. J. Karlsson, E. Landemark, Y. C. Chao, and R. I. G. Uhrberg, *Phys. Rev. B* **45**, 6321 (1992).

⁹J. N. Andersen, O. Björneholm, A. Sandell, R. Nyholm, J. Forsell, L. Thånell, A. Nilsson, and N. Mårtensson, *Synchrotron Radiat. News* **4**, 15 (1991).

¹⁰G. LeLay, M. Göthelid, T. M. Grehk, M. Björkqvist, V. Yu. Aristov, and U. O. Karlsson, *Phys. Rev. B* **50**, 14 277 (1994).

¹¹T. M. Grehk, M. Björkqvist, M. Göthelid, G. LeLay, and U. O. Karlsson (unpublished).

¹²C. Törnevik *et al.* (unpublished).

¹³W. Ewald, *J. Appl. Phys.* **25**, 1436 (1954).

¹⁴*Constitution of Binary Alloys*, edited by M. Hansen (McGraw-Hill, New York, 1958).

¹⁵E. Cohen and A. K. W. A. van Lieshout, *Proc. Acad. Sci. Amsterdam* **40**, 746 (1936).